Journal of MECHANICAL ENGINEERING – Strojnícky časopis,
VOL 68 (2018), NO 4, 65 - 74

ALL-PASS FILTERS IN THE SYSTEMS OF ACTIVE VIBRATION CONTROL OF WEAKLY-DAMPED SYSTEMS

TŮMA Jiří[1], ŠURÁNEK Pavel[1], ŽIARAN Stanislav[2]

[1]*Faculty of Mechanical Engineering, VSB – the Technical University of Ostrava, Department of Control Systems and Instrumentation, 17. listopadu 15, 708 33 Ostrava, Czech Republic, e – mail: jiri.tuma@vsb.cz*
[2]*Faculty of Mechanical Engineering, Slovak University of Technology in Bratislava, Institute of Applied Mechanics and Mechatronics, Nám. Slobody 17,812 31 Bratislava, Slovakia*

Abstract: The problem of active vibration control of weakly damped mechanical structures is potentially unstable modes of vibrations due to the positive feedback for some vibration modes. The paper will discuss the change of positive feedback on the negative one using all-pass discrete-time filters. These filters can be arranged in a cascade to stabilize many potentially unstable modes. The piezoelectric actuator as a source of force is used to damp vibration.

KEYWORDS: active vibration control; all-pass filter; piezo-actuator

1 Introduction

The problem of the active vibration control of weakly-damped mechanical structures consists of potentially unstable modes of vibrations. For the increase of the gain feedback, some of the poles of the transfer function in the complex plane recede the stability boundary which is the imaginary axis, while the other poles approach it. For a large feedback gain, these poles cross the stability boundary, and the system becomes unstable. In this case, the feedback becomes positive for these vibration modes. The paper will discuss the change of positive feedback on the negative one using all-pass discrete-time filters. Arranging these filters in a cascade is possible. The piezoelectric actuator as a source of force is used to damp vibration. The problem is that this actuator type has a hysteresis which has to be taken into account when analyzing the effect of active vibration control. Simulation examples will illustrate the theory.

2 Model of the flexible mechanical structure

As assumed, the paper deal with the mechanical systems of N degrees of freedom. The response of these mechanical systems to external forces describes the equation of motion in a matrix form

$$\mathbf{M}\ddot{\mathbf{y}} + \mathbf{C}\dot{\mathbf{y}} + \mathbf{K}\mathbf{y} = \mathbf{F} \tag{1}$$

where $\mathbf{M}$, $\mathbf{C}$, and $\mathbf{K}$ denote the mass, damping, and stiffness matrices, respectively, $\mathbf{F}$, $\mathbf{y}$, $\dot{\mathbf{y}}$, and $\ddot{\mathbf{y}}$ are the force, linear displacement, velocity and acceleration vectors, respectively. Note that matrices $\mathbf{M}$, $\mathbf{C}$, and $\mathbf{K}$ are square symmetric of the size $N \times N$. The linear displacement can be considered as a coordinate and refers to a specific node of the mechanical system. An additional term on the left side of the equation of motion that is proportional to the velocity vector indicates the presence of viscous damping as a dissipative force. The damping matrix is assumed to be of the Rayleigh type $\mathbf{C} = \alpha\mathbf{M} + \beta\mathbf{K}$, where α, β are the constants of

DOI: 10.2478/scjme-2018-0048, Print ISSN 0039-2472, On-line ISSN 2450-5471

proportionality. The dependence of the damping ratio ξ on frequency f in hertz yields from the formula $\xi = \pi(\alpha/f + \beta f)$. The numerical value of the constants of proportionality is as follows $= 0.159\ [s^{-1}],\ \beta = 0.0000411\ [s]$.

By solving the equation $(\mathbf{K} - \omega_k^2\mathbf{M})\mathbf{u}_k = \mathbf{0}$ where a vector $\mathbf{u}_k$ is known in mathematics as an eigenvector, we obtain the vibration frequency ω_k of the undamped system. The number of solutions is equal to N, and all column eigenvectors form a matrix $\mathbf{U}$. Since arbitrary nonzero factors scale the eigenvectors, we must normalize them to make them unique. The normalized eigenvectors form the modal matrix $\mathbf{V} = [\mathbf{v}_1, \mathbf{v}_2, \dots, \mathbf{v}_N]$. Normalization of the matrix of eigenvectors has to fulfill the equation $\mathbf{V}^T\mathbf{M}\mathbf{V} = \mathbf{I}$, where $\mathbf{I}$ is the matrix of identity.

The external forces $\mathbf{F} = [F_1, F_2, \dots, F_N]$ are the inputs of the mechanical system and displacement $\mathbf{y} = [y_1, y_2, \dots, y_N]^T$ are its outputs. The matrix $\mathbf{H}$ which entries $H_{r,q}(\omega)$ relate the force acting at the node indexed by q to the displacement y_r is a transfer matrix. The individual entries of the matrix $\mathbf{H}$ as a function of the angular frequency ω are as follows

$$H_{r,q}(\omega) = \sum_{n=1}^{N} \frac{v_{n,r}v_{n,q}}{\Omega_n^2 - \omega^2 + j2\xi_n\Omega_n\omega}\ ,\quad r,q = 1,2,\dots,N \tag{2}$$

where $v_{n,r}v_{n,q}, n, r, q = 1, \dots, N$ are the elements of the N-dimensional normalized eigenvector $\mathbf{v}_n = \left[v_{n,1}, v_{n,2}, \dots, v_{n,N}\right]^T$ which is associated with the natural frequency Ω_n and the relative damping ξ_n. The coordinates $v_{n,1}, v_{n,2}, \dots, v_{n,N}$ determine a vibration or mode shape. The transfer function (2) of the system is a sum of the transfer functions of the second order systems which correspond to the vibration mode indexed by n. The product $k_n = v_{n,r}v_{n,q}$ for the given value of indexes r and q is called a modal constant and depends on the modal shapes for the natural frequency Ω_n. The modal constant plays a critical role in the type of feedback.

3 Model of the cantilever beam

This paper deals with active vibration control of the cantilever beams. Fig. 1 defines the coordinates and dimensions of the vibrating structure. The beam is divided into N elements. As the motion is assumed only in the direction of y, therefore the degree of freedom is equal to N.

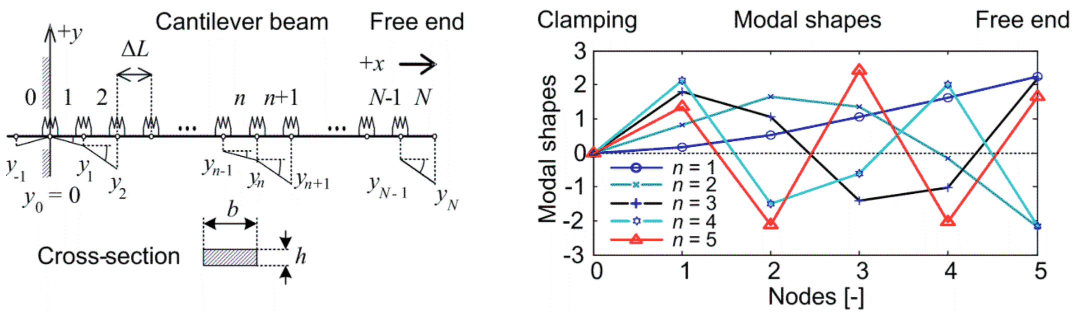

Fig. 1 Coordinates and elements of a cantilever beam, modal shapes

The stiffness and mass matrices for the cantilever beam have been derived in the preceding publications [1, 2, 3, 4, 5, 6]. For calculation of the stiffness matrix, a bending stiffness of the beam plays an important role. This stiffness K_δ relates the applied bending moment Q to the resulting rotation $\Delta\delta$ of the elementary beam

$$K_\delta = Q/\Delta\delta \tag{3}$$

where $E = 2.14 \times 10^{11} [N/m^2]$ is Young's modulus of the beam material, $I_z = bh^3/12$ is the area moment of inertia of the beam cross-section concerning the axis which is perpendicular to the *xy*-plane.

The stiffness and mass matrix has the following form

$$\mathbf{K} = \frac{K_\delta}{\Delta L^3}\begin{bmatrix} 7 & -4 & 1 & & & & & & \\ & & \vdots & \vdots & \vdots & \vdots & \vdots & & \\ & & 1 & -4 & 6 & -4 & 1 & & \\ & & \vdots & \vdots & \vdots & \vdots & \vdots & & \\ & & & & & & 1 & -2 & 1 \end{bmatrix}, \quad \mathbf{M} = \begin{bmatrix} B & A & & & & & & & \\ & & \vdots & \vdots & \vdots & \vdots & \vdots & & \\ & & & A & B & A & & & \\ & & \vdots & \vdots & \vdots & \vdots & \vdots & & \\ & & & & & & & A & B/2 \end{bmatrix} \tag{4}$$

where parameters A and B of the mass matrix are as follows

$$A = \frac{\Delta m}{4}\left\{1 - \frac{1}{3}\left[1 + \left(\frac{h}{\Delta L}\right)^2\right]\right\}, \qquad B = \frac{\Delta m}{2}\left\{1 + \frac{1}{3}\left[1 + \left(\frac{h}{\Delta L}\right)^2\right]\right\} \tag{5}$$

For simulation study a beam with the following parameters is used: length L = 0.5 [m], width b = 0.04 [m], and thickness h = 0.005 [m]. In this case, the beam is divided into N = 5 elements. All the natural frequencies are shown in Table 1 and corresponding modal shapes on the right side of Fig. 1.

Table 1 Modal frequencies

Mode	1	2	3	4	5
Frequency [Hz]	19.03	114.3	308.3	575.3	842.5

As is apparent from the modal shapes in Fig. 2, the signs of the modal constants are as follows

$$v_{1,5}v_{1,1} > 0, v_{2,5}v_{2,1} < 0, v_{3,5}v_{3,1} > 0, v_{4,5}v_{4,1} < 0, v_{5,5}v_{5,1} > 0$$

For vibration modes with the index equal to an odd integer, the modal constants are positive while for the even index the modal constant is negative.

The equation of motion (1) is the second order ordinary differential equation. After the introduction of the substitution of $\mathbf{u}_1 = \mathbf{y}$ and $\mathbf{u}_2 = \dot{\mathbf{y}}$, the second order equation represents two differential equations of the first order. An arrangement of the subsystem which models the beam for any number of elements in the Matlab-Simulink is shown in Fig. 2. Entering the simulation is complete to the initial conditions $\mathbf{u}_1(0) = \mathbf{y}(0)$, and $\mathbf{u}_2(0) = \dot{\mathbf{y}}(0)$. The blocks of the *Gain* type contain the product of the matrix and the vector, and therefore the output is a vector as well.

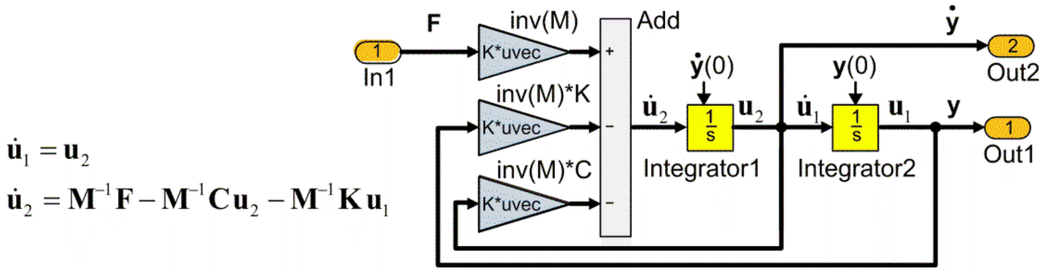

Fig. 2 Matlab-Simulink model of the beam

4 Piezo-actuator in the closed-loop

Piezo-actuators generate force or displacement (travel, stroke) which depends on the electrical supply voltage. The relationship between force and displacement describes the working graph which is shown on the left side of Fig. 3. The supply voltage determines each curve of this figure. The nominal displacement L_{max} for the maximum supply voltage V_{max}

and the blocking force F_{max} specify the technical data of the actuator, or it can be found by measurements. The blocking force is the maximum force generated by the actuator at the maximum supply voltage and zero travel [7]. Because we use the stacked LVPZT (low voltage PZT type) piezoelectric actuator of the P-844.60 type originated from the PI Company, the catalogue specification of this piezo-actuator is used to plot the working graph in Fig. 3.

The piezo-actuator generates the force F of the magnitude according to the formula as follows

$$F = F_{max}(V/V_{max} - L/L_{max}) \tag{6}$$

The travel of the piezo-actuator is equal to the deflection of the beam at the node where the piezo-actuator operates. The piezo-actuator travel equals the length $L = -y_r$ isThe piezo-actuator has a finite stiffness which results from the nominal displacement and the blocking force as follows

$$K_P = F_{max}/LV_{max} = 3000\ [N]/0.0000\ [m] = 33\ [MNm^{-1}] \tag{7}$$

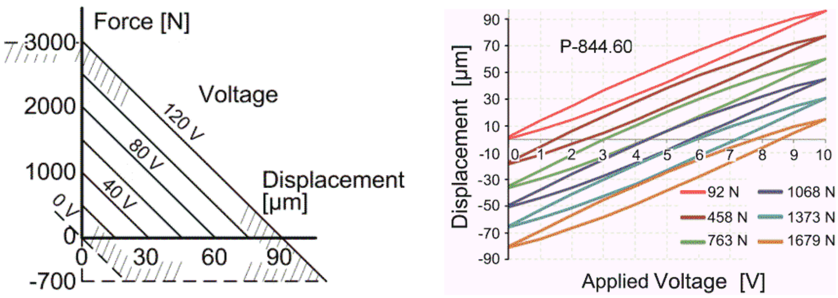

Fig. 3 Working graph for the P-844.60 piezo-actuator and hysteresis measurements

The piezo-actuator exhibits significant hysteresis. The result of the hysteresis measurements is shown on the right side of Fig. 3. This data originates from doctoral theses of J. Los [8]. Each loop corresponds to the constant loading force acting on the piezo-actuator in its rise and fall. There are several ways how to create a model of hysteresis. For example, a model according to Prandtl-Ishlinskii is based on a backlash in a mechanism. The *Backlash* block of Matlab-Simulink implements a system in which a change in input causes an equal change in output. However, when the input changes direction, an initial change in input does not affect the output which remains at the previous value. The principle of the piecewise approximation of the output displacement on the input control voltage is shown on the left side of Fig. 4. This diagram also explains the meaning of the parameters that are constant inputs for the other blocks of Matlab-Simulink while the diagram on the right side of this figure shows the result of simulation with the use of 11 *Backlash* blocks. The dissertation contains a detailed description of the calculation of parameters g and w [8, 9, 10].

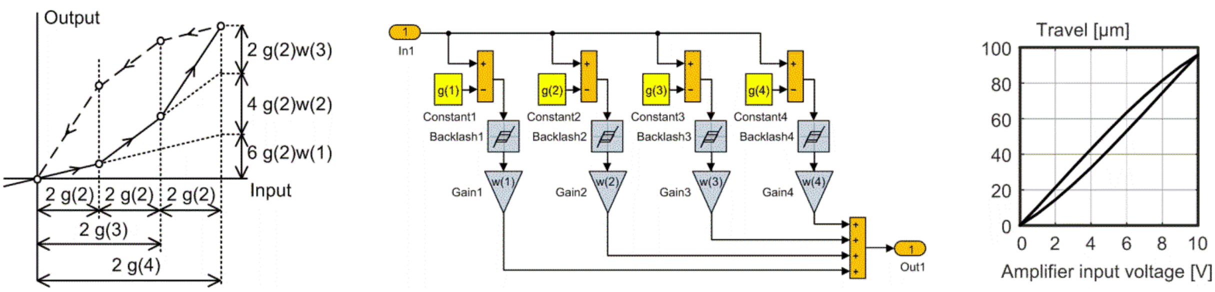

Fig. 4 Prandtl-Ishlinskii model of hysteresis

Just as there are two ways of modelling electric power sources according to the Thévenin theorem and the dual Norton theorem also piezo-actuators can be modelled similarly, i.e. either as a source of force F^* or as a source of displacement y^* with the connection of the inner spring which simulates the piezo-actuator stiffness K_P and is calculated according to (7). Both the solutions are shown in Fig. 5 [8]. In these diagrams, the force is equivalent to the electric current and displacement to the electric voltage. The force acting on the beam must be corrected taking into account the piezo-actuator stiffness in both cases as is shown in Fig. 5.

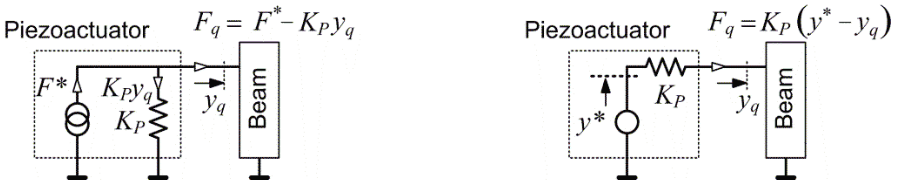

Fig. 5 Two ways of connection of piezo-actuator and beam models

Connecting the piezo-actuator to the beam changes the natural frequencies of the complete system in the same way. The effect of the piezo-actuator stiffness on the stiffness matrix for the left equivalent in Fig. 5 can be determined by the same procedure as was created the equation of motion of the beam with the use of the Lagrange's equations. The deflection of the piezo-actuator spring determines the potential energy, and after the partial derivative concerning the coordinate of the node q, we found the effect of its stiffness on the elements of the matrix **K**. The stiffness of the piezo-actuator increases the magnitude of the main diagonal elements of the stiffness matrix **K** which is indexed by q. We add the piezo-actuator stiffness to one element on the main diagonal of the stiffness matrix. The actual resonant frequencies for the case where the piezo-actuator is a part of the beam structure shows Table 2. An example of the Frequency Response Function (FRF) $j\omega H_{5,1}(\omega)$ for the input of the force acting at node #1 and the output which is a velocity (change rate of y_5) at the node #5 is shown on the left side of in Fig. 6. The velocity signal $\dot{y}_S$ is a feedback of the control loop for active vibration control.

Table 2 Modal frequencies of the complex system

Mode	1	2	3	4	5
Frequency [Hz]	24.1	155.3	437.8	790.1	2976.7

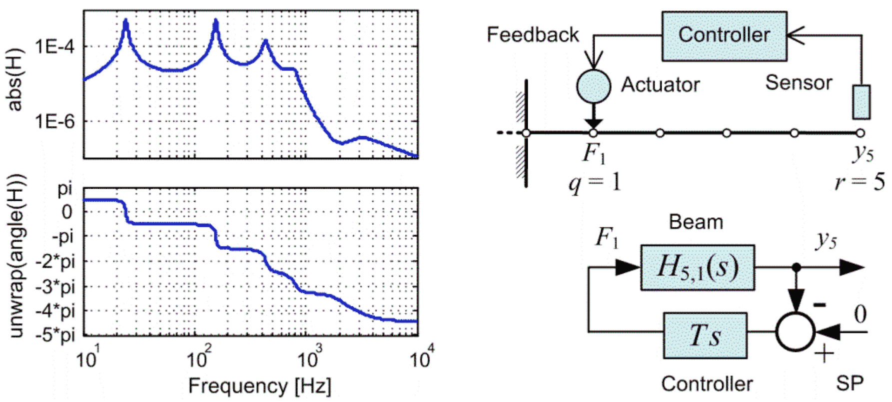

Fig. 6 Frequency response function $j\omega H_{5,1}(\omega)$ and the AVC system of the cantilever beam

The magnitude of FRF shows the resonant frequency peaks corresponding to the vibration modes. The resonant amplification for the first and second mode is achieved hundredfold greater compared to the gain in the background of FRF. The modal constants for these natural frequencies have approximately the same absolute value but the opposite sign. The feedback effects are contradictory on the stability. It is important that the resonant peaks are well separated, i.e., between them is the gap between the amplification of oscillations and the second frequency is nearly a hundred times greater.

5 Active vibration control

The purpose of the system for the active vibration control (AVC) is to compensate the effect of a disturbing external force on the vibration of the mechanical structure. The assessment of the damping effect of AVC specifies changes in displacement, velocity or acceleration of the selected node of the structure. It can be the free end of the cantilever beam which models a cutting tool or boring bar of the lathe for instance. The result of the active dumping is the minimum motion around the steady-state position and the minimum velocity or acceleration of vibrations.

There are two possible solutions, the collocated and non-collocated active vibration control. For the collocated system, the correcting force acts at the same node where we detect the response of the mechanical structure. For the non-collocated system, we assume that the correcting force acts at the node indexed by q and we detect the vibrations at the node indexed by $r \neq q$. An example of the non-collocated system is shown on the right side of Fig. 6. We sense the vibration of the free end element of this cantilever beam at the node $r = 5$, and the correcting force acts at the element just next to the clamped end, therefore $q = 1$.

Mechanical structures are weakly damped. Theoretical analysis shows that for undamped systems there are absent terms of the odd powers of the complex variables s in the Laplace transfer function. The undamped system is at the margin of stability. It has been shown that the most appropriate controller for such systems uses proportional feedback based on the velocity change of the controlled displacement as is shown on the right side of Fig. 6. The controller is a derivative type regarding displacement as a controlled variable. The setpoint (SP) for such a closed-loop system is equal to zero. The gain of the velocity feedback is designated by T. The stability of the feedback system determines the position of the pole of the closed-loop transfer function. The beam is a stable system without control due to the natural damping; it does not start to vibrate by itself. The increase of the feedback gain causes that one of the poles associated with the two lowest resonant frequencies moves away from the instability margin in the complex plane in the left direction while the other pole is approaching or exceeding the stability margin. For the given beam, which is divided into five elements, and the assumption of the Rayleigh's damping, the locus of the closed-loop transfer function poles are shown in Fig. 7. The root locus demonstrates the effect of the derivative controller time constant T change on the system stability. The time constant varies from 0 to 1E6. The location of the poles of the transfer function calculates the Matlab function called root as the roots of the polynomial $1 + TsH_{5,1}(s)$.

Because the degree of polynomial equals ten in the complex variable s, the number of roots, i.e., the number of poles is ten as well. Five pairs of poles are complex conjugate. The stability margin crosses the pole for the mode $n = 2$ and the pole for the mode $n = 4$ approaches this margin.

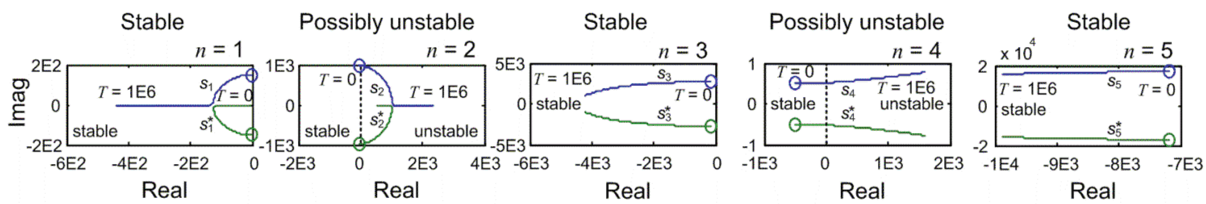

Fig. 7 Root locus to demonstrate the effect of the time constant T change

The analysis shows that the opposite sign of the modal constants reduces the damping effect of velocity feedback. There are two possible ways how to improve the efficiency of the active vibration control of weakly damped systems

- either control each vibration mode separately
- or change the positive feedback to the negative one.

Both the methods indicate the transition of the controller design from the frequency range from zero to infinity to the control in a narrow frequency band.

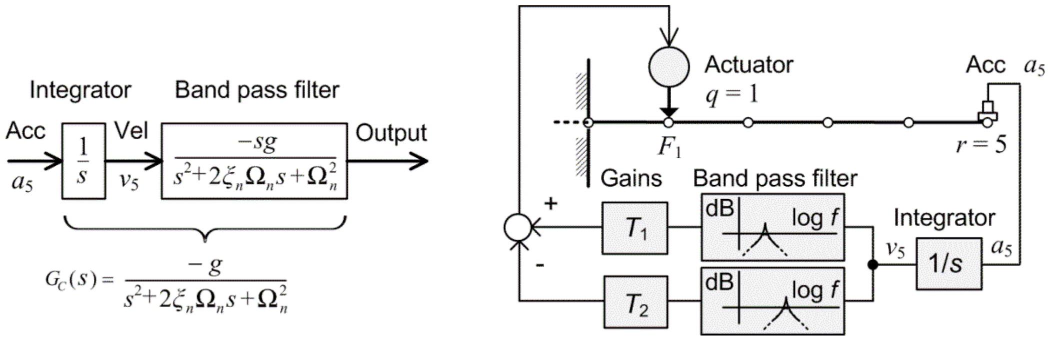

Fig. 8 Principle of Positive Position Feedback (PPF)

The first possible solution with the filter of the band-pass type is shown in Fig. 8. This arrangement of the AVC system is called a Positive Position Feedback (PPF) controller [11]. In the mentioned figure, the method of PPF solves the problem of two resonant frequencies, one of them corresponds to the negative feedback and the second one corresponds to the positive feedback. The input signal of the filter is a signal of the velocity type. The proportional controller connected to the filter output only amplifies this signal. We obtain the velocity signal to connect it to the filter input by integrating the acceleration signal with respect to time. We consider the acceleration on the free end of the beam as the controlled variable. The integration and band-pass filtering together form a low-pass filter, whose transfer function has been designed previously by many authors and it was a topic of the doctoral theses defended by P. Šuránek [12]. The filter is of the second order and therefore causes the least possible delay in the control loop. The properties of the closed loop can be adjusted by the gain of the proportional controller which operates in the narrow frequency band around the resonant frequency.

The second method for controlling the weakly damped systems is converting the positive feedback to negative with the use of an all-pass filter. This type of the frequency filter modifies the phase of the harmonic signal at the output compared to the input without changing the amplitude of the signal frequency components. The filter of this type of the first-order type changes the phase from 0 to π radians in the frequency range from 0 to infinity. The all-pass filter of the second order shown on the left and middle of Fig. 9 doubles the phase change. For the possibly unstable modes, it is necessary to change the phase by π at the resonant frequency of this vibration mode whose modal constant is to be changed from the negative to positive value. The advantage of this filter is the controllable rate of the change of phase concerning the change of the frequency by setting the value of the relative damping parameter ξ_{APF}.

$$G_{APF,n}(s) = \frac{s^2 - 2\xi_{APF}\,\omega_n\,s + \omega_n^2}{s^2 + 2\xi_{APF}\,\omega_n\,s + \omega_n^2}$$

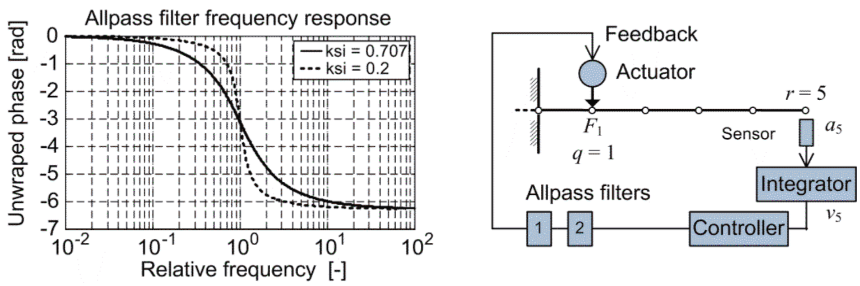

Fig. 9 All-pass filter frequency response (ksi = ξ_{APF}).

Since $|G_{APF\,n}(j\omega)| = 1$ only a phase frequency response for two values of the damping parameter ξ_{APF} is shown in the middle of Fig. 9. The all-pass filters are connected in series (cascade) with the controller as it is shown on the right of Fig. 9. The count of these filters is as many as the count of the negative modal constants.

6 Simulation results

The effect of the all-pass filter on the damping of the beam vibration demonstrates the control system responses with the use of the two all-pass filters in the closed loop and without them as is shown on the right of Fig. 9. The first all-pass filter is tuned to the frequency of the second vibration mode, and the second one to the frequency of the fourth vibration mode. The beam is excited by a short pulse after 1 second from the beginning of the simulation. During 1 second, the piezo-actuator is gradually prestressed by the force of 1500 N. The decaying vibration response without any active vibration control (AVC OFF) is shown on the left of Fig. 10. The effect of ACV without using the all-pass filter (ALL-PASS FILTER OFF) is shown in Fig. 6. Due to the stability, the open-loop gain can be set less or equal to 4. The serial connection of two all-pass filters in the cascade allows increasing the gain of the open-loop in such a way that the time constant T may be increased up to the value of 25 but less than 30 with correspondingly increasing the damping effect as is shown on the right of Fig. 10. The result of the experiment for the acceleration of the beam free end is shown in Fig. 11. The beam has the same dimensions as in the simulation study.

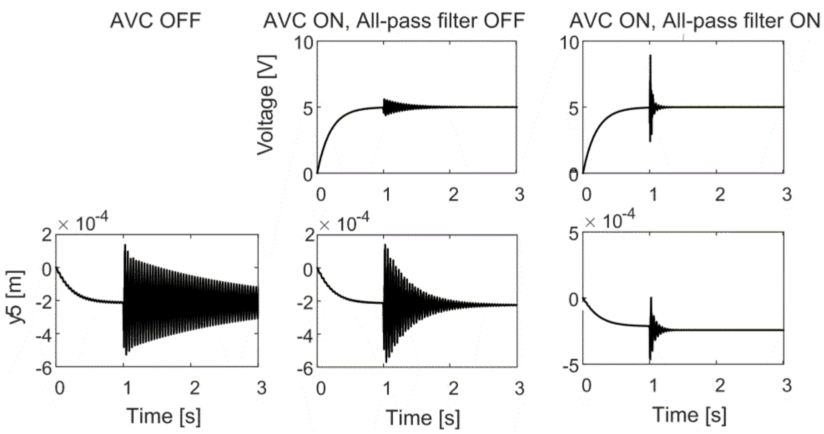

Fig. 10 Decaying vibration without any active control and two ways of the active vibration controls

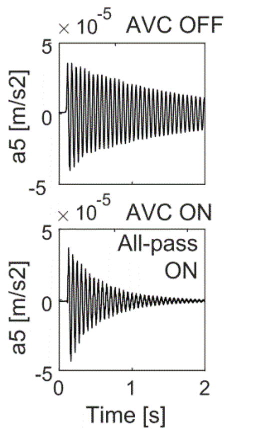

Fig. 11 Experiment

7 CONCLUSION

The Matlab-Simulink model of the cantilever beam was designed using the method based on the modal analysis. In addition to the beam model, an active vibration control model using piezo-actuators was created. Because piezo-actuators have considerable hysteresis, the Prandtl-Ishlinskii model of hysteresis based on a backlash in a mechanism complements the model of the complex control system. Mechanical systems are usually weakly damped. Conventional methods of controller synthesis are not suitable for the design of active damping of weakly-damped systems. Some modes for these systems become potentially unstable when increasing the gain of the closed loop. The paper describes the method that converts the positive feedback to the negative feedback using the all-pass filter. For comparison, the PPF method is also described. The effect of the all-pass filter method on increasing the damping by shortening the impulse response has been verified by simulation and experimental approach.

ACKNOWLEDGMENT

Authors thank to the European Regional Development Fund in the Research Centre of Advanced Mechatronic Systems project No. CZ.02.1.01/0.0/0.0/16_019/0000867 within the Operational Programme Research, Development and Education and also thank to the R&D in the project No. SP2018/123.

REFERENCES

[1] J. Tůma, J. Škutová. Simulation of active vibration control of the cantilever. Proceedings of the 13th International Carpathian Control Conference (ICCC 2012), May 28 - 31 **2012**, High Tatras; Slovakia, 744 – 747. ISBN: 978-1-4577-1868-7

[2] P. Šuránek, M. Mahdal, J. Tůma, and J. Zavadil. Modal analysis of the cantilever beam. Proceedings of the 14th International Carpathian Control Conference (ICCC 2013), May 26 - 29 **2013**, Rytro, Poland, 367 – 372. ISBN: 978-1-4673-4490-6

[3] P. Šuránek, M. Mahdal, J. Tůma. Modelling and Simulation of an Active Damped Structure, In 15th International Carpathian Control Conference (ICCC 2014), 28-30 May **2014**, Velké Karlovice, Czech Republic. ISBN: 978-1-4799-3527-7

[4] J. Tůma, P. Šuránek, M. Mahdal. Vibration damping of the cantilever beam with the use of the parametric excitation, In: Proceedings of the 21st International Congress on Sound and Vibration (ICSV 21), 13-17 July **2014**, Beijing, China. Paper 905.

[5] J. Tůma, P. Šuránek, M. Mahdal, R. Wagnerová. Linear piezo-actuators in systems of the active vibration control, In: Proceedings of the 23rd International Congress on Sound and Vibration (ICSV 23), 10-14 July **2016**, Athens Greece.

[6] R. Jančo, L. Ėcsi, P. Ėlesztős. FSW Numerical Simulation of Aluminium Plates by Sysweld - Part I. *Journal of Mechanical Engineering – Strojnícky časopis* **2016** (66), No. 1, 47 – 52.

[7] S. O. Reza Moheimani, A. J. Fleming. Piezoelectric Transducers for Vibration Control and Damping. Springer, **2006**. ISBN-13:9781846283314

[8] L. Los. Mechatronic systems with piezo-actuators (Mechatronické systémy s piezoaktuátory – in Czech), Doctoral thesis, VSB – Technical University of Ostrava, **2016**.

[9] P. Staňák, J. Sládek, V. Sládek. Analysis of Piezoelectric Semiconducting Solids by Meshless Method. *Journal of Mechanical Engineering – Strojnícky časopis* **2016** (65), No. 1, 77 – 92.

[10] A. Buchacz, M. Płaczek, A. Wrobel. Modelling and analysis of systems with cylindrical piezoelectric transducers. *Mechanika* **2014** (20), No. 1, 87 –91.

[11] A. Preumont. Active vibration control of active structures : an introduction. Kluwer Academic Publishers, **1997**.

[12] P. Šuranek, Active vibration control (Aktivní potlačování vibrací – in Czech), Doctoral thesis, VSB – Technical University of Ostrava, **2016**.